

*Supporting Information*

**Fabrication of Metallic Nickel-Cobalt Phosphide Hollow Microspheres for  
High-Rate Supercapacitors**

Miao Gao,<sup>†</sup> Wei-Kang Wang,<sup>†</sup> Xing Zhang, Jun Jiang\*, Han-Qing Yu\*

CAS Key Laboratory of Urban Pollutant Conversion, Department of Applied Chemistry,

University of Science & Technology of China, Hefei, 230026, China

<sup>†</sup> These authors contributed equally to this work.

**\* Corresponding author:**

Dr. Jun Jiang, Fax: +86-551-63602449; E-mail: [junj@ustc.edu.cn](mailto:junj@ustc.edu.cn)

Prof. Han-Qing Yu, Fax: +86-551-63601592; E-mail: [hqyu@ustc.edu.cn](mailto:hqyu@ustc.edu.cn).

**Materials and Reagents.** Nickel nitrate hexahydrate ( $\text{Ni}(\text{NO}_3)_2 \cdot 6\text{H}_2\text{O}$ ), cobalt nitrate hexahydrate ( $\text{Co}(\text{NO}_3)_2 \cdot 6\text{H}_2\text{O}$ ), urea, ethanol, sodium hypophosphite ( $\text{NaH}_2\text{PO}_2$ ) and KOH were purchased from Sinopharm Chemical Reagent Co., China. Nickel foam was supplied by Chang-An Metal Material Co., China. All materials were used without further purification.

**Physicochemical Characterization.** The X-ray power diffraction (XRD) patterns of the samples were obtained on a Philips X' Pert PRO SUPER diffractometer equipped with graphite monochromatized Cu K $\alpha$  radiation ( $\lambda = 1.541874 \text{ \AA}$ ). The scanning electron microscopy (SEM) images of the samples were taken with an X-650 scanning electron micro analyzer and a JSM-6700F field emission SEM (JEOL Co., Japan). The transmission electron microscopy (TEM) images of the samples were recorded on a TEM (JEM-2100, JEOL Co., Japan) using an electron kinetic energy of 200 kV. The high-resolution transmission electron microscopy (HRTEM) images and selected area electron diffraction (SAED) patterns were taken on an HRTEM (2010, JEOL Co., Japan) at an acceleration voltage of 200 kV. High angle annular dark field scanning transmission electron microscopy (HAADF-STEM) images and the corresponding energy dispersive spectroscopic (EDS) mapping analyses were performed by using TEM/STEM with a spherical aberration corrector (Talos F200X, FEI Co., USA). The chemical compositions and the valence states of constituent elements were analyzed by X-ray photoelectron spectroscopy (XPS) (ESCALAB250, Thermo Fisher Inc., USA). The surface area was measured by using the Brunauer–Emmett–Teller (BET) method with a Builder 4200

instrument (Tristar II 3020M, Micromeritics Co., USA).

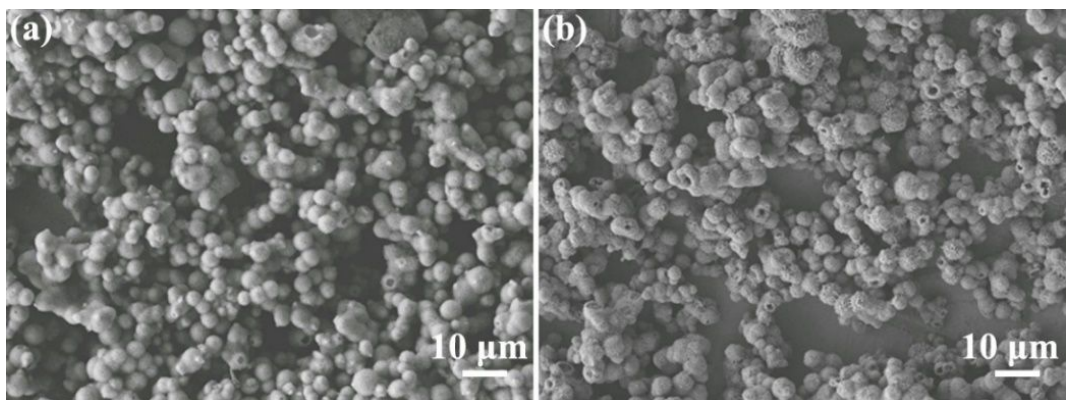


**Figure S1.** SEM images of (a) NiCoCH, and (b) urchin-like NiCoP hollow spheres.

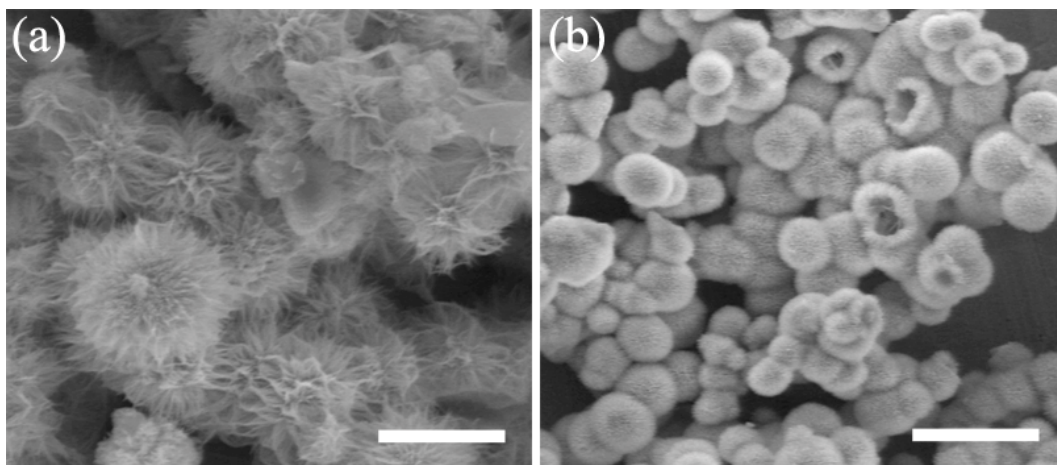


**Figure S2.** SEM images of the products obtained with different amounts of urea: (a) less: 0.18 g, and (b) more: 1.5 g. Scale bar: 2  $\mu\text{m}$ .

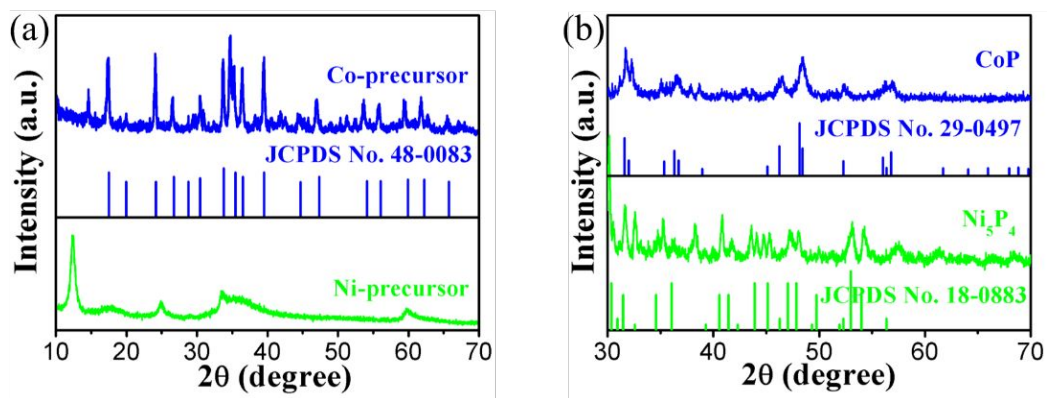


**Figure S3.** Power XRD patterns of (a) Co-precursor and Ni-precursor, and (b) CoP and Ni<sub>5</sub>P<sub>4</sub>.

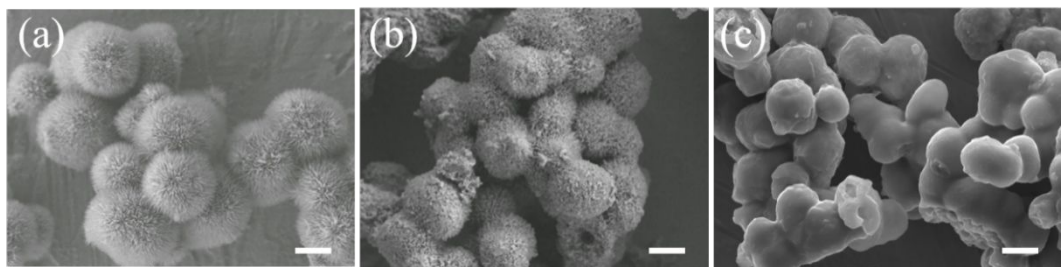


**Figure S4.** SEM images of the products obtained with different amounts of  $\text{NaH}_2\text{PO}_2$ : (a) 1:5, (b) 1:15, and (c) 1:20. Scale bar: 2  $\mu\text{m}$ .

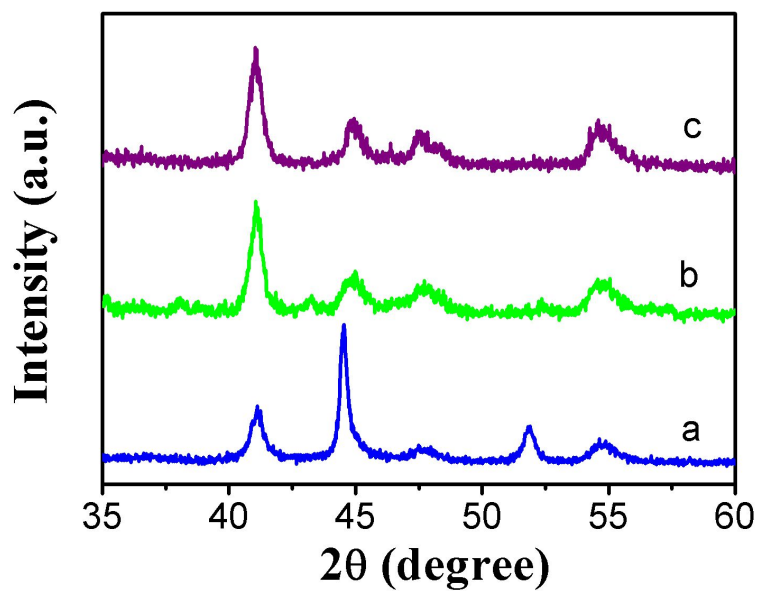


**Figure S5.** Power XRD patterns of the products obtained with different amounts of  $\text{NaH}_2\text{PO}_2$ : (a) 1:5, (b) 1:15, and (c) 1:20.



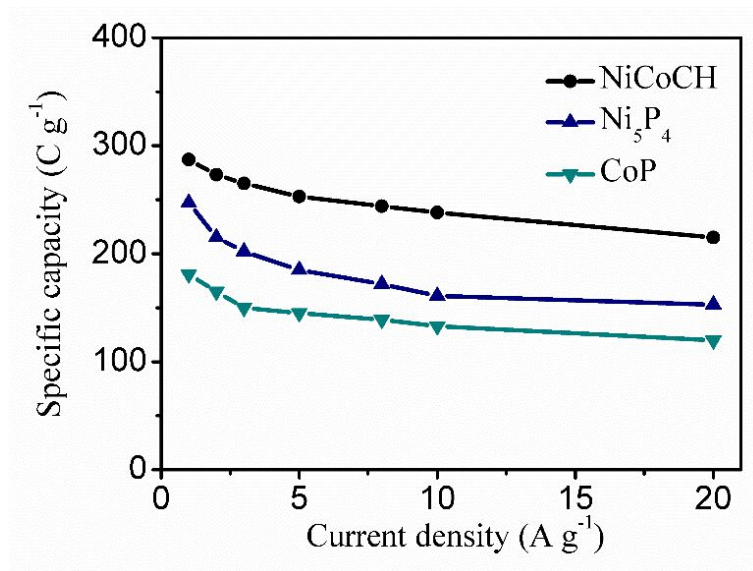


**Figure S6.** Specific capacities of NiCoCH, Ni<sub>5</sub>P<sub>4</sub> and CoP electrodes as a function of current densities.

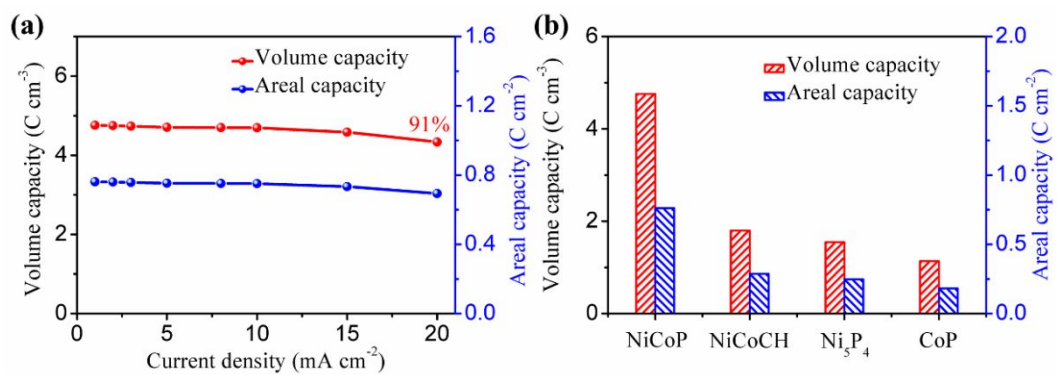


**Figure S7.** (a) Volume and areal capacities of NiCoP at different current densities. (b)

Volume and areal capacities of NiCoP, NiCoCH,  $\text{Ni}_5\text{P}_4$  and CoP at 1  $\text{mA cm}^{-2}$ .

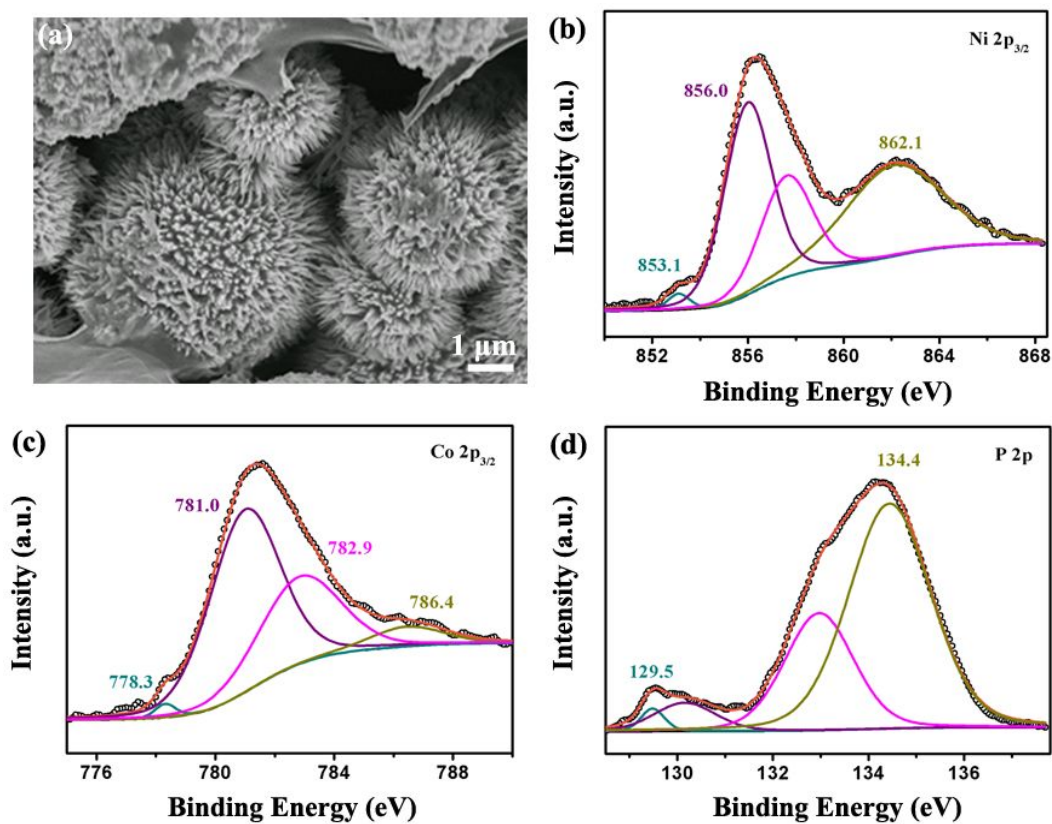


**Figure S8.** (a) SEM image after 5000 cycles, and XPS spectra of (b) Ni 2p, (c) Co 2p, and (d) P 2p of NiCoP after 5000 cycles.

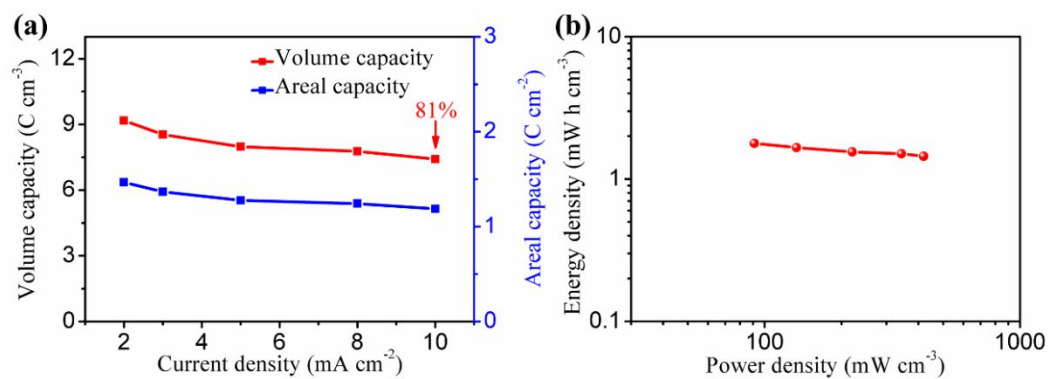


**Figure S9.** (a) Volume and areal capacities of NiCoP//AC hybrid supercapacitors at different current densities. (b) Ragone plot of the device.

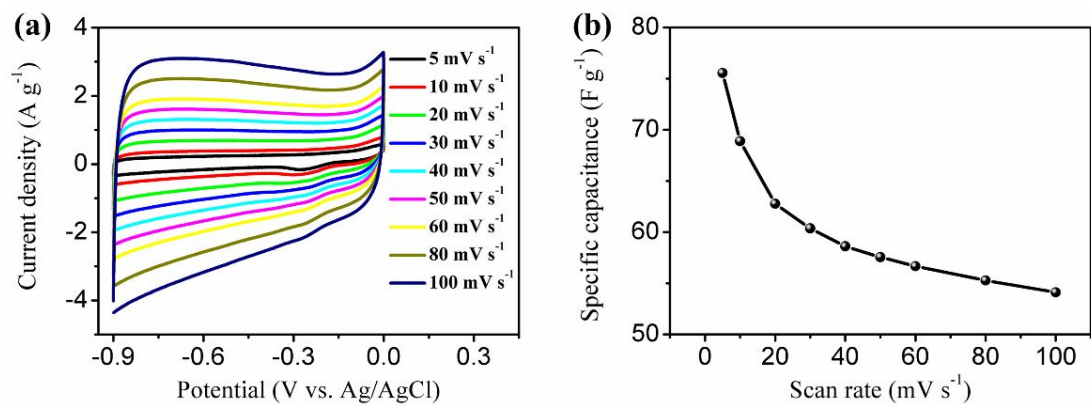


**Figure S10.** (a) CV curves of active carbon at different scan rates, and (b) the corresponding specific capacitances.

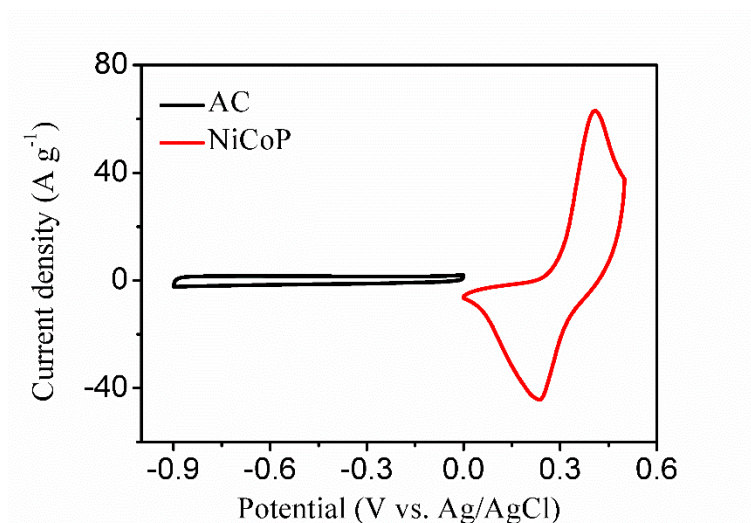


**Figure S11.** CV curves of AC and NiCoP electrodes at 50 mV s<sup>-1</sup>.

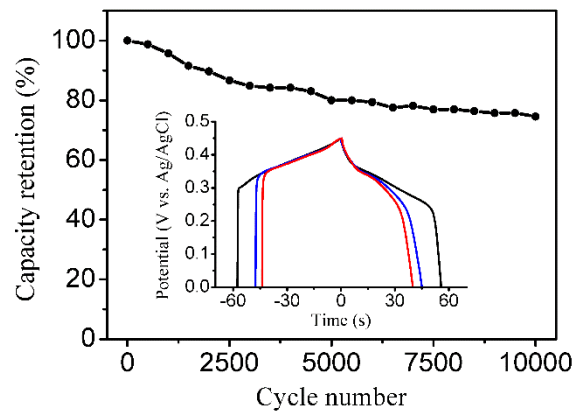


**Figure S12.** Cycling stability of NiCoP electrode at a current density of  $10 \text{ A g}^{-1}$  for 10000 cycles.

**Table S1** Comparison in the Electrochemical Performance of Ni, Co-Based Materials

Material	Capacitance retention (%)	Electrolyte (aqueous)	Ref.
Carbon nanotube foams/Co(OH) <sub>2</sub>	0.5→10 A g <sup>-1</sup> 72.4%	2 M KOH	1
ZnCo <sub>2</sub> O <sub>4</sub> @ Ni <sub>x</sub> Co <sub>2x</sub> (OH) <sub>6x</sub>	5→50 mA cm <sup>-2</sup> 60.6%	2 M KOH	2
Ni <sub>2</sub> P	1→8 A g <sup>-1</sup> 76.3%	2 M KOH	3
Ni <sub>5</sub> P <sub>4</sub>	1→8 A g <sup>-1</sup> 55.9%	2 M KOH	3
Ni <sub>2</sub> P NS/NF	2.5→83.3 A g <sup>-1</sup> 31.7%	6 M KOH	4
Co <sub>3</sub> O <sub>4</sub> @ Ni(OH) <sub>2</sub> NAs	1→20 A g <sup>-1</sup> 70.4%	6 M KOH	5
ZnCo <sub>2</sub> O <sub>4</sub>	2→10 A g <sup>-1</sup> 39.5%	2 M KOH	6
Ni@Ni(OH) <sub>2</sub>	1→10 A g <sup>-1</sup> 35.6%	1 M KOH	7
NiCo <sub>2</sub> O <sub>4</sub> NSs@ HNRs	5→100 mV s <sup>-1</sup> 45.71%	1 M KOH	8
NiCoP	1→20 A g <sup>-1</sup> 91.1%	1 M KOH	This work



## REFERENCES

- (1) Wang, C.; Qu, H.; Peng, T.; Mei, K.; Qiu, Y.; Lu, Y.; Luo, Y.; Yu, B., Large Scale Alpha-Co(OH)<sub>2</sub> Needle Arrays Grown on Carbon Nanotube Foams as Free Standing Electrodes for Supercapacitors. *Electrochim. Acta* **2016**, *191*, 133-141.
- (2) Fu, W.; Wang, Y.; Han, W.; Zhang, Z.; Zha, H.; Xie, E., Construction of Hierarchical ZnCo<sub>2</sub>O<sub>4</sub>@Ni<sub>x</sub>Co<sub>2x</sub>(OH)<sub>6x</sub> Core/Shell Nanowire Arrays for High-Performance Supercapacitors. *J. Mater. Chem. A* **2016**, *4*, 173-182.
- (3) Wang, D.; Kong, L. B.; Liu, M. C.; Luo, Y. C.; Kang, L., An Approach to Preparing Ni-P with Different Phases for Use as Supercapacitor Electrode Materials. *Chemistry* **2015**, *21*, 17897-903.
- (4) Zhou, K.; Zhou, W.; Yang, L.; Lu, J.; Cheng, S.; Mai, W.; Tang, Z.; Li, L.; Chen, S., Ultrahigh-Performance Pseudocapacitor Electrodes Based on Transition Metal Phosphide Nanosheets Array via Phosphorization: A General and Effective Approach. *Adv. Funct. Mater.* **2015**, *25*, 7530-7538.
- (5) Zhang, X.; Xiao, J.; Zhang, X.; Meng, Y.; Xiao, D., Three-Dimensional Co<sub>3</sub>O<sub>4</sub> Nanowires@Amorphous Ni(OH)<sub>2</sub> Ultrathin Nanosheets Hierarchical Structure for Electrochemical Energy Storage. *Electrochim. Acta* **2016**, *191*, 758-766.
- (6) Zhang, D.; Zhang, Y.; Li, X.; Luo, Y.; Huang, H.; Wang, J.; Chu, P. K., Self-Assembly of Mesoporous ZnCo<sub>2</sub>O<sub>4</sub> Nanomaterials: Density Functional Theory Calculation and Flexible All-Solid-State Energy Storage. *J. Mater. Chem. A* **2016**, *4*, 568-577.
- (7) Su, Y. Z.; Xiao, K.; Li, N.; Liu, Z. Q.; Qiao, S. Z., Amorphous Ni(OH)<sub>2</sub>@Three-Dimensional Ni Core-Shell Nanostructures for High Capacitance Pseudocapacitors and Asymmetric Supercapacitors. *J. Mater. Chem. A* **2014**, *2*, 13845-13853.
- (8) Lu, X. F.; Wu, D. J.; Li, R. Z.; Li, Q.; Ye, S. H.; Tong, Y. X.; Li, G. R., Hierarchical NiCo<sub>2</sub>O<sub>4</sub> Nanosheets@Hollow Microrod Arrays for High-Performance Asymmetric Supercapacitors. *J. Mater. Chem. A* **2014**, *2*, 4706-4713.